

# Faraday ghosts: depolarization canals in the Galactic radio emission

Anvar Shukurov<sup>\*†</sup> and Elly M. Berkhuijsen<sup>\*</sup>

*Max-Planck-Institut für Radioastronomie, Auf dem Hügel 69, Bonn D-53121, Germany*

Accepted ... . Received ...; in original form ...

## ABSTRACT

Narrow, elongated regions of very low polarized intensity – so-called canals – have recently been observed by several authors at decimeter wavelengths in various directions in the Milky Way, but their origin remains enigmatic. We show that the canals arise from depolarization by differential Faraday rotation in the interstellar medium and that they represent level lines of Faraday rotation measure RM, a random function of position in the sky. Statistical properties of the separation of canals depend on the autocorrelation function of RM, and so provide a useful tool for studies of interstellar turbulence.

**Key words:** magnetic fields – polarization – turbulence – ISM : magnetic fields

## 1 INTRODUCTION

Radio polarization maps of the Milky Way often exhibit a network of apparently randomly oriented, narrow (less than the beam width), elongated regions where polarized intensity vanishes or is greatly reduced. These structures, now known as ‘canals’, have been reported by a number of authors and belong to the class of structures visible in polarized emission that do not have counterparts in the total radio intensity (Duncan et al. 1997; Gray et al. 1998, 1999; Uyaniker et al. 1999a; Haverkorn, Katgert & de Bruyn 2000; Gaensler et al. 2001). In Fig. 1 we show an example of canals in the field of the nearby galaxy M31. Some of the canals are nearly closed, forming cells, or at least have pronounced curvature, and within the cells the polarization angle often hardly varies. Other canals are more or less straight, and often occur in nearly parallel pairs. The appearance of the canals depends on the wavelength of observation (Haverkorn et al. 2000). An example of similar features was discussed by Scheuer, Hannay & Hargrave (1977).

The canals were first identified as distinct features in polarization maps by Duncan et al. (1997) and Uyaniker et al. (1999a). The latter authors propose that the canals may be caused by filaments in thermal plasma and/or suitable magnetic structures. As shown by Haverkorn et al. (2000), the polarization angle of the radio emission flips by about  $90^\circ$  across a canal, which prompted these authors to suggest that the canals arise from beam depolarization due to a

discontinuous distribution of the foreground Faraday rotation measure RM caused by abrupt changes in the magnetic field direction. Gaensler et al. (2001) support the idea of beam depolarization, but note that the foreground RM does not exhibit abrupt changes across the canals, and therefore attribute these structures to a highly nonuniform magnetic field in the synchrotron source. It seems, however, highly implausible that the distribution of magnetic field should be discontinuous to that extent, and that either the variations of RM have just the right amplitude to rotate the polarization angle preferentially by  $90^\circ$  or the magnetic field direction changes preferentially by right angles. Furthermore, neither of these interpretations can easily explain why the pattern of canals changes with wavelength.

The canals apparent in the field of M31 (see Fig. 1) must originate in the Milky Way because their network extends far beyond the image of M31. An eyeball estimate of the typical separation of the canals is about  $5'$ , corresponding to a linear scale of about 1 pc at a distance of 1 kpc. Figure 1b confirms that the polarization angles flip by about  $90^\circ$  across the canals.

Uyaniker et al. (1998; 1999a) mention the possibility that the canals may be due to Faraday depolarization without giving any details. We attribute the canals to depolarization along the line of sight rather than across the beam. This was first proposed by Beck (1999; 2001) who showed that the canals can arise from depolarization by differential Faraday rotation, and so do not require any discontinuities or even strong gradients in the parameters of the interstellar medium (ISM). In this letter we substantiate this idea and argue that the canals represent level lines of RM where  $RM = RM_0 \equiv n\pi/(2\lambda^2)$  with  $\lambda$  the wavelength and  $n = 1, 2, 3, \dots$ . Then we discuss how statistical properties of

\* E-mail: anvar.shukurov@ncl.ac.uk (AS); eberkhuijsen@mpifr-bonn.mpg.de (EMB)

† On leave from the Department of Mathematics, University of Newcastle, NE1 7RU, U.K.

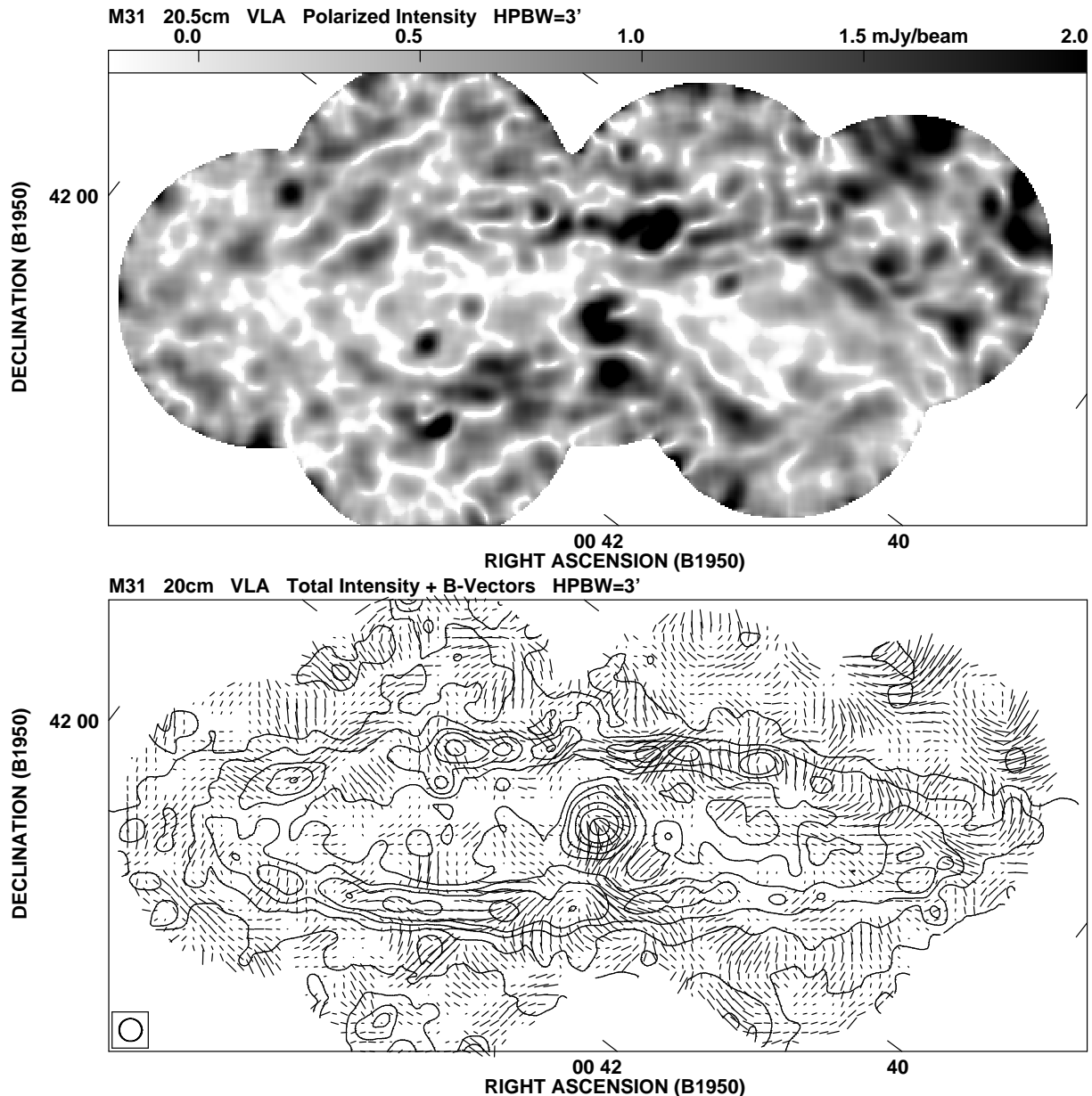


**Figure 1.** (a) Polarized intensity at  $\lambda 20.5$  cm in the field of the galaxy M31, obtained by smoothing the high-resolution map of Beck, Berkhuijsen & Hoernes (1998) to an angular resolution of  $3'$  (no corrections for missed spacings were made). The frame measures  $130' \times 60'$  with the major axis of M31 oriented horizontally, and is centred on the nucleus at Galactic coordinates  $(l, b) \approx (120^\circ, -20^\circ)$ . Because of strong depolarization, polarized emission from M31 is only visible as slight enhancements of emission along a large, elliptical ring and near the nucleus, better visible in total intensity in (b). Canals are visible as an irregular network of narrow, low-intensity regions (light shades of grey). As this network extends to the borders of the map, i.e. to regions outside of M31, the canals and much of the polarized emission must originate in the Milky Way. (b) The distribution of the  $B$ -vectors of polarized emission (observed  $E$ -vectors rotated by  $90^\circ$ ) at  $\lambda 20.5$  cm in the field of M31 shown in (a). The angular resolution of  $3'$  is indicated in the lower left corner. The length of the vectors is proportional to the polarized intensity with  $3'$  corresponding to  $2$  mJy/beam area. The canals seen in (a) are visible as narrow lanes (less than  $3'$  wide) that are free of vectors. Note the sudden changes in the polarization angle by about  $90^\circ$  across the canals. Contour levels of 5, 10, 15, 20, 30, 40 and 60 mJy/beam area show the total power emission from M31 at  $\lambda 20.5$  cm.

the ISM can be determined from the angular separation of the canals.

## 2 DIFFERENTIAL FARADAY ROTATION

Differential Faraday rotation is one of the simplest and best known depolarization mechanisms which arises where rela-

tivistic and thermal electrons fill the same region of magnetized medium, so that synchrotron emission and Faraday rotation occur together. The degree of polarization  $p$  then varies with the observable Faraday rotation measure RM and  $\lambda$  as (Burn 1966, Sokoloff et al. 1998)

$$p = p_0 \frac{\sin |2RM\lambda^2|}{|2RM\lambda^2|}, \quad (1)$$

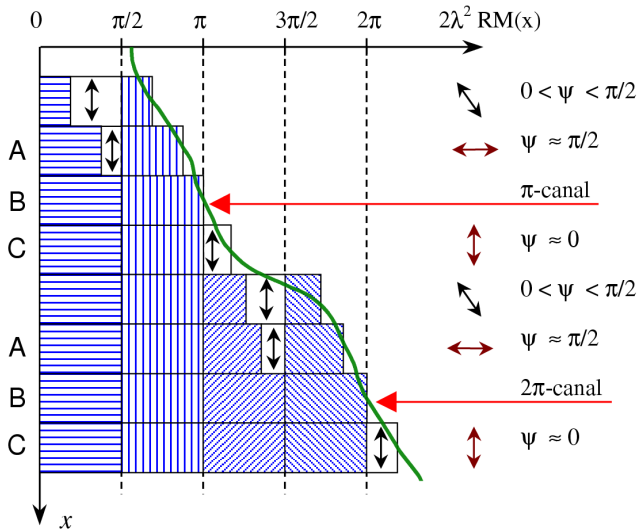


**Figure 2.** Differential Faraday rotation under a range of intrinsic Faraday rotation measures. Each horizontal strip represents one telescope beam with the observer to the right; the continuous curve represents the function  $2\lambda^2 \text{RM}(x)$  that varies across the sky (along  $x$ ); the intrinsic polarization angle is uniform (vertical double arrows on the left). Emission generated in a layer where the former is rotated by  $\pi/2$ , i.e., where  $2\lambda^2 \text{RM}(x) = \pi/2$ . Regions whose emissions mutually cancel are indicated by perpendicularly hatched boxes. Only the emission from unshaded regions reaches the observer. The arrows on the right show the observed polarization plane which has been Faraday rotated in layers to the right of the visible (unshaded) region to give the polarization angle  $\psi$  in the range indicated. Note that layers to the right of the source act as a Faraday screen, and so the rotation angle is  $2\lambda^2 \text{RM}$ . The canals occur where the polarized emission is fully cancelled (regions labelled B). The emission observed at values of  $2\lambda^2 \text{RM}(x)$  slightly smaller than  $n\pi$  (regions A) and slightly larger than  $n\pi$  (regions C) originate in different layers. The difference in  $2\lambda^2 \text{RM}(x)$  between regions A and C is  $\pi/2$ . Therefore, emission from region A is rotated by  $\pi/2$  before reaching the observer, whereas emission from region C is rotated only slightly. Thus, the polarization angles observed on the two sides of a canal differ by  $\pi/2$ . A canal that occurs when  $2\lambda^2 \text{RM}(x) = n\pi$  with  $n = 1$  is shown near the top, and with  $n = 2$ , near the bottom.

and so vanishes when  $|\text{RM}| = \text{RM}_0$ , where

$$2\text{RM}_0\lambda^2 = \pi n, \quad n = 1, 2, \dots, \quad (2)$$

with  $p_0 \approx 0.75$  the intrinsic degree of polarization. This expression is applicable to a uniform slab and to a few more complicated configurations discussed by Sokoloff et al. (1998), and is sufficient for our purposes here. It is important to note that the angle of polarization suffers jumps by  $\pi/2$  at the same values of RM where  $p$  vanishes [see, e.g., Fig. 2b in Burn (1966) and Sect. 3.1 in Sokoloff et al. (1998)]. The nature of depolarization by differential Faraday rotation and the origin of the jumps are further illustrated in Fig. 2.

If RM varies across the sky, polarized intensity will vanish at those positions  $\mathbf{x}$  in the sky plane where  $2|\text{RM}(\mathbf{x})|\lambda^2 = \pi n$ , i.e., for a given wavelength, at the critical level lines of RM where  $|\text{RM}(\mathbf{x})| = \text{RM}_0$ . For example,  $\text{RM}_0 \approx 37n \text{ rad m}^{-2}$  for  $\lambda = 20.5 \text{ cm}$ . The loci of vanishing polarization are geometric lines, i.e., they are infinitely thin, hence always narrower than the beam, as are the canals

(Gaensler et al. 2001; see Fig. 1a). The position of the level lines changes with wavelength, as does the network of canals. Extended polarized emissions seen on different sides of a canal come from different regions along the line of sight (see Fig. 2). Hence, the polarization angles differ by  $\pi/2$  as RM crosses the critical level  $\text{RM}_0$ , i.e., across the canal. Faraday depolarization does not affect the total synchrotron emission, so canals are not visible in total intensity. We believe that these arguments are convincing enough to attribute the canals to depolarization by differential Faraday rotation. As they are not directly related to any structures in the ISM, we call them ‘Faraday ghosts’.

We now recall that in the turbulent interstellar medium RM is a random function of the position. As discussed by Wardle & Kronberg (1974) and Naghizadeh-Khouei & Clarke (1993), the probability distribution function of the observed polarization angle is well approximated by a Gaussian as long as the Stokes parameters are Gaussian random variables and the signal-to-noise ratio is large enough. Since the Faraday rotation measure between two wavelengths is proportional to the difference of the polarization angles, RM is also a Gaussian random function. According to our estimates, the deviations from the Gaussian distribution in RM do not exceed a few percent for signal-to-noise ratios exceeding unity. In Fig. 1a the signal-to-noise ratio is larger than 3 (Beck et al. 1998).

### 3 LEVEL LINES OF A RANDOM FUNCTION

It is useful to distinguish two types of level lines of a random distribution of RM, and so two types of canals. Level lines of the first type occur at a level close to the mean value of RM, denoted here  $\overline{\text{RM}}$ , whereas the others occur near high, rare peaks of RM. The two types have distinct statistical properties.

Consider a random function of position  $F(\mathbf{x})$ , with  $\sigma_F$  its standard deviation,  $\sigma_F^2 = \langle [F(\mathbf{x}) - \overline{F}]^2 \rangle$ , where angular brackets denote averaging,  $\overline{F} = \langle F(\mathbf{x}) \rangle$  the mean value of  $F(\mathbf{x})$ , and  $C(r)$  its normalized autocorrelation function,

$$\sigma_F^2 C(r) = \langle F(\mathbf{x})F(\mathbf{x} + \mathbf{r}) \rangle - \overline{F}^2, \quad r = |\mathbf{r}|,$$

where  $F(\mathbf{x})$  has been assumed to be statistically homogeneous, so the autocorrelation function depends on  $r$  alone.

#### 3.1 Passages through a level $F_0$

Now consider positions where  $F(\mathbf{x})$  passes through a certain level  $F_0$  that does not differ much from the mean value of  $F$ , i.e.,  $|\overline{F} - F_0| \simeq \sigma_F$  (as we discuss below, this is the case in Fig. 1). The corresponding canals will form cells where they surround local extrema of  $F(\mathbf{x})$  or will have low curvature, like a contour of constant height along a valley or a mountain ridge.

A useful summary of the theory of passages of a random function  $F(\mathbf{x})$  through a level  $F_0$  can be found in Sect. 33 of Sveshnikov (1965). The theory applies to both Gaussian and non-Gaussian random fields, but here we only present results for the Gaussian case. The total probability of both upward and downward passages is given by

$$P(F_0) = \frac{1}{\pi} \frac{\sigma_{\nabla F}}{\sigma_F} \exp \left[ -\frac{(F_0 - \overline{F})^2}{2\sigma_F^2} \right], \quad (3)$$

where  $\sigma_{\nabla F}$  is the standard deviation of the spatial derivative of  $F(\mathbf{x})$ . The mean number of the level lines per unit length is simply given by  $n_0 = P(F_0)$ . Since  $\sigma_{\nabla F}^2/\sigma_F^2 = -d^2C(r)/dr^2|_{r=0} = 2/l_T^2$ , where  $l_T$  is known as the Taylor microscale (e.g., Sect. 6.4 in Tennekes & Lumley 1972), this yields the following expression for the mean separation of level lines:

$$\overline{x}_0 = n_0^{-1} = \frac{\pi}{\sqrt{2}} l_T \exp \left[ \frac{(F_0 - \overline{F})^2}{2\sigma_F^2} \right]. \quad (4)$$

In application to the level lines of RM discussed below, one should allow for passages through both the levels  $+F_0$  and  $-F_0$  because the canals occur wherever  $|\text{RM}| = \text{RM}_0$ . Then Eq. (3) contains an additional term on the right-hand side, proportional to  $\exp[-(F_0 + \overline{F})^2/2\sigma_F^2]$ . This term can be significant if  $\overline{F} \approx 0$ .

### 3.2 Level lines around high peaks

In this section we consider level lines that occur near high extrema of  $F(\mathbf{x})$  and so tend to be closed lines enclosing a relatively small region, like a contour of constant height near a high mountain peak. In the astrophysical context, statistics of high peaks have been explored in studies of structure formation by gravitational instability in a random density field (Peebles 1984; Bardeen et al. 1986).

Consider the neighbourhood of a position where  $F(\mathbf{x})$  has a high peak, and assume that  $F(\mathbf{x}) > 0$ . For convenience, let this position be  $\mathbf{x} = 0$ , so that  $\nabla F(0) = 0$  and  $F(0) = \nu\sigma_F$ , where  $\nu (\gg 1)$  is the dimensionless height of the peak. Then  $F(\mathbf{x})$  at a given  $\mathbf{x}$  near the peak is a random variable. The main result useful for our purposes is that, for a Gaussian random function, the distribution of  $F(\mathbf{x})$  is Gaussian with the mean value

$$\langle |F(\mathbf{r}) - \overline{F}| \rangle = F(0)C(r), \quad (5)$$

where  $r$  is the distance from the peak. In other words, the mean profile of a Gaussian random function near a high peak is given by its autocorrelation function. Then the distance of the level line from the peak,  $r_0$ , follows from Eq. (5) with  $\langle |F(\mathbf{r}) - \overline{F}| \rangle = |F_0 - \overline{F}|$  and  $C(r) = C(r_0)$ .

Assuming that the autocorrelation function has a power-law form in the relevant range of scales,  $C(r) = 1 - Ar^\mu$  with certain constants  $A$  and  $\mu$  ( $\mu > 0$ ), we obtain the following expression for the mean separation of the level lines,  $\overline{x}_0 = 2r_0$ :

$$\overline{x}_0 = 2 \left[ \frac{1}{A} \left( 1 - \frac{|F_0 - \overline{F}|}{\nu\sigma_F} \right) \right]^{1/\mu}. \quad (6)$$

## 4 THE MEAN ANGULAR SEPARATION OF CANALS

The application of the above results is straightforward. Now  $F = |\text{RM}(\mathbf{x})|$ , where  $\mathbf{x}$  is position in the plane of the sky. Equations (4) and (6) with  $\overline{F} = |\overline{\text{RM}}|$  and  $\text{RM}_0 = n\pi/(2\lambda^2)$  show that the angular separation of the canals depends on the mean value and standard deviation of RM, and on  $\lambda$ , via

$$\frac{|F_0 - \overline{F}|}{\sigma_F} = \frac{|n\pi/2\lambda^2 - |\overline{\text{RM}}||}{\sigma_{\text{RM}}}.$$

According to Eq. (4),  $\overline{x}_0$  decreases as  $\lambda$  grows for  $\lambda^2 < n\pi/(2|\overline{\text{RM}}|)$  and increases at larger  $\lambda$ . Interestingly, Eq. (6) shows the opposite behaviour.

To discuss the properties of the canals, we use the map of Fig. 1 where the canals are very prominent and where we can obtain reliable estimates of  $\overline{\text{RM}}$  and  $\sigma_{\text{RM}}$ . The mean value of RM in the direction of M31, obtained from the rotation measures of extragalactic radio sources in that part of the sky, is  $\text{RM}_{\text{fg}} \simeq -90 \text{ rad m}^{-2}$  (Beck 1982; Han, Beck & Berkhuijsen 1998). This value of RM, produced in the Galactic foreground, can be identified with the intrinsic Faraday rotation measure, or the Faraday depth in that direction,  $0.81 \int_0^L n_e B_{\parallel} ds$  with  $n_e$  the electron density,  $B_{\parallel}$  the line-of-sight magnetic field component, and  $L$  the pathlength through the magneto-ionic medium. However, for polarized emission arising within the Milky Way the maximum observable RM would be  $\frac{1}{2}\text{RM}_{\text{fg}}$  if polarized emission from all distances through the Milky Way were visible (because of differential Faraday rotation). The observable RM can be further reduced by depolarization. Then RM that enters Eq. (1) is just a part of  $\frac{1}{2}\text{RM}_{\text{fg}}$ . An estimate of the depth through the Milky Way over which the observed polarized emission is produced and the corresponding effective value of  $\overline{\text{RM}}$  can be obtained as follows.

The dominant mechanism of depolarization, apart from differential Faraday rotation, is internal Faraday dispersion due to turbulence in the ISM. The standard deviation of RM in the field of M31 calculated between  $\lambda 6 \text{ cm}$  and  $\lambda 11 \text{ cm}$  is  $\sigma_{\text{RM}} \simeq 10 \text{ rad m}^{-2}$  at a scale of  $5'$  (Berkhuijsen et al. 2003). Using Eq. (34) of Sokoloff et al. (1998), we conclude that this mechanism reduces the degree of polarization at  $\lambda 20.5 \text{ cm}$  by about 16%. Therefore, the effective geometric depth visible at this wavelength is about 0.84 of the path length through the magneto-ionic layer of the Milky Way in that direction. (Thus, the region visible in polarized emission at  $\lambda 20.5 \text{ cm}$  in the direction of M31 is about 2 kpc deep, assuming that the scale height of the magneto-ionic layer is 0.8 kpc.) Then the observable Faraday rotation measure produced within the Milky Way at  $\lambda 20.5 \text{ cm}$  can be estimated as

$$\overline{\text{RM}} \simeq \frac{1}{2} 0.84 \text{RM}_{\text{fg}} \simeq -38 \text{ rad m}^{-2}.$$

The smallest value of RM at which complete depolarization occurs at  $\lambda = 20.5 \text{ cm}$  is  $\text{RM}_0 \approx 37 \text{ rad m}^{-2}$  from Eq. (2). Since  $\text{RM}_0 - |\overline{\text{RM}}|$  is even smaller than  $\sigma_{\text{RM}}$ , results of Sect. 3.1 apply and Eq. (4) yields  $\overline{x}_0 \simeq 2.2l_T$  for the mean separation of canals. Our estimate of the mean separation of canals in Fig. 1 gave  $\overline{x}_0 \simeq 5'$ , resulting in  $l_T \simeq 2'$ . This result is discussed in Sect. 5.

A useful diagnostic of the effects discussed here is the displacement of the canals as  $\lambda$  changes so that  $\text{RM}_0$  of Eq. (2) changes by  $\Delta \text{RM}_0 \ll \text{RM}_0$ . Equation (4) yields the following estimate for the relative displacement of a canal (equal to half the increment in  $\overline{x}_0$ ):

$$\frac{\Delta x}{\overline{x}_0} \simeq \Delta \text{RM}_0 \frac{|\text{RM}_0 - |\overline{\text{RM}}||}{2\sigma_{\text{RM}}^2},$$

where we have neglected terms quadratic in  $\Delta \text{RM}_0$ . For the observations of Gaensler et al. (2001) where  $|\overline{\text{RM}}| \simeq -13 \text{ rad m}^{-2}$ ,  $\sigma_{\text{RM}} \simeq 45 \text{ rad m}^{-2}$  (B. Gaensler, private com-

munication) and  $\Delta\text{RM}_0 \approx 4.8 \text{ rad m}^{-2}$ , we obtain  $\Delta x/\bar{x}_0 \approx 0.024$ . We estimate the typical separation of canals in the maps of Gaensler et al. as  $\bar{x}_0 \approx 7'$ , which yields  $\Delta x \approx 0.2'$ , i.e., about 1/6 of the beam width in these observations.

Alternatively, the displacement of an individual canal between wavelengths  $\lambda_1$  and  $\lambda_2$  can be estimated if the gradient of RM,  $\nabla\text{RM}$ , is known as  $\Delta x = \frac{1}{2}\pi(\lambda_1^{-2} - \lambda_2^{-2})|\nabla\text{RM}|^{-1}$ . For the observations of Haverkorn et al. (2000), where RM varies by about  $5 \text{ rad m}^{-2}$  across the beam width of  $4'$ , we obtain  $\Delta x \approx 0.3'$ , i.e., less than 10% of the beam width.

For the sake of illustration, let us estimate the separation of canals that occur near high peaks of  $|\text{RM}|$ . Since  $\text{RM}_0 - |\overline{\text{RM}}| \lesssim \sigma_{\text{RM}}$  in the field of M31 at  $\lambda 20.5 \text{ cm}$ , the theory described in Sect. 3.2 is not useful here and we scale the result to  $\lambda 11 \text{ cm}$ . Minter & Spangler (1996) suggest the following form of the structure function of RM fluctuations in the directions around  $(l, b) = (144^\circ, -21^\circ)$ , i.e., not far from the field shown in Fig. 1:  $D(r) \simeq 5910 r^{5/3} \text{ rad}^2 \text{ m}^{-4}$  at  $r \lesssim 0.14$  ( $\approx 8'$ ), with  $r$  the angular separation in degrees. With  $C(r) = 1 - D(r)/(2\sigma_{\text{RM}}^2)$ , Eq. (6) yields for Fig. 1:

$$\frac{\bar{x}_0}{5'} \simeq 2 \left\{ \frac{\sigma_{\text{RM}}^2}{47 \text{ rad}^2 \text{ m}^{-4}} \left[ 1 - \frac{130 \text{ rad m}^{-2}}{\nu \sigma_{\text{RM}}} \right] \times \left| n \left( \frac{0.11 \text{ m}}{\lambda} \right)^2 - \frac{|\overline{\text{RM}}|}{130 \text{ rad m}^{-2}} \right| \right\}^{3/5}. \quad (7)$$

## 5 DISCUSSION

As shown above, the mean separation of canals in Fig. 1 is related to the Taylor microscale, a measure of the curvature of the autocorrelation function of RM at small separations. In the present context, the Taylor microscale can be tentatively identified, e.g., with the thickness of magnetic ropes, or with the size of blobs or the thickness of filaments in the thermal electron distribution. We emphasize that the canals are *not* directly related to any ropes or filaments in the magneto-ionic medium. However, the statistical properties of the canals are sensitive to small-scale structures in the medium. Ropy structures of magnetic fields arise naturally from fluctuation dynamo action (Zeldovich, Ruzmaikin & Sokoloff 1990; Subramanian 1999), and filamentary structures in the gas components are abundant in the ISM (e.g., Koo, Heiles & Reach 1992). The resulting estimate of the rope thickness,  $2'$ , corresponds to about 0.6 pc at a distance of 1 kpc. Faraday rotation from such structures would be difficult to observe directly as they would need to have  $n_e B_{\parallel} \gtrsim 20 \mu\text{G cm}^{-3}$  in order to produce  $|\text{RM}| \gtrsim \sigma_{\text{RM}} \simeq 10 \text{ rad m}^{-2}$ .

When combined with Faraday dispersion, depolarization by differential Faraday rotation leads to a smooth dependence of  $p$  on RM, where  $p$  does not entirely vanish at the local minima (Sokoloff et al. 1998). This leads to canals where polarized intensity does not vanish but is only strongly reduced; still, they preserve, in an approximate manner, the properties discussed above.

Canals have been observed in many directions in the Milky Way. In particular, Duncan et al. (1997) have detected them at the wavelength  $\lambda 12.6 \text{ cm}$  in the southern Galactic plane. As follows from Eq. (2), the value of  $\text{RM}_0$  at that

wavelength is at least  $100 \text{ rad m}^{-2}$ , and so the canals are observed because the mean Faraday rotation measure is suitably high in that direction.

A signature of the mechanism discussed here is the displacement of the canals when the wavelength varies. Canals produced by discontinuities in magnetic field or Faraday rotation measure would not shift with wavelength, whereas those produced by differential Faraday rotation must shift as described in Sect. 4. However, canal displacements consistent with our model may be too small to be detected in the data available.

Another interesting type of ghosts in polarized emission is discussed by Gaensler et al. (2001). These ghosts arise in interferometer observations because an extended, polarized (and unpolarized) background, uniform in intensity (to which an interferometer is insensitive), is missing. However, small-scale structures in polarization angle (i.e., in the Stokes parameters  $Q$  and  $U$ ) are not missed and cause variations in the observed polarized intensity but not in the total synchrotron intensity. This can result in blobs and filaments of enhanced or reduced polarized intensity. These effects may lead to extreme fractional polarization, possibly even above 0.75. Wieringa et al. (1993) describe polarized filaments invisible in total intensity, observed with the Westerbork interferometer. We note that ghosts of this type also occur in single-dish observations (Uyaniker et al. 1999a). Except for some fields of Uyaniker et al. (1999a), such measurements are rarely absolutely calibrated in both total and polarized intensities. Therefore, a baselevel is subtracted to obtain a zero level for the emission. Such ghosts may be called ‘*base-level ghosts*’. Furthermore, missing spacings and baselevel corrections have the same effect as a missing (i.e., depolarized) quasi-uniform, magneto-ionic layer. They lead to a shift in the positions of the canals and possibly to their (dis)appearance, without changing their statistical nature. As base-level ghosts can be produced at one’s will in any data by adjusting the zero level, this opens new possibilities to study the magneto-ionic medium using the ghosts.

In summary, both Faraday ghosts (canals) and base-level ghosts (blobs, depressions, filaments) are features in the observed polarized emission without a counterpart in the total emission. As they do not arise from any real structures in the ISM, we call them ‘ghosts’. The canals are due to depolarization by differential Faraday rotation in the turbulent magneto-ionic medium. They are signs of the turbulent structure of the ISM over a range of scales, and so represent a useful probe of interstellar turbulence.

## ACKNOWLEDGMENTS

We have benefited from numerous discussions with R. Beck, who also kindly produced Fig. 1. We are grateful to B. Gaensler, D. Moss, I. Patrickeyev, W. Reich, D. D. Sokoloff, K. Subramanian, B. Uyaniker and R. Wielebinski for useful discussions and suggestions. This work was supported by the NATO collaborative research grant CRG1530959 and PPARC Grant PPA/G/S/1997/00284. AS is grateful to R. Wielebinski for hospitality at the MPIfR.

**REFERENCES**

- Bardeen J. M., Bond J. R., Kaiser N., Szalay, A. S., 1986, *ApJ*, 304, 15
- Beck R., 1982, *A&A*, 106, 121
- Beck R., 1999, in Berkhuijsen E. M., ed., *Galactic Foreground Polarization*. MPIfR, Bonn, p. 3
- Beck R., 2001, *Space Sci. Rev.*, 99, 243
- Beck R., Berkhuijsen E. M., Hoernes P., 1998, *A&AS*, 129, 329
- Berkhuijsen E. M., Beck R., Hoernes P., 2003, *A&A* (in press)
- Burn, B. J., 1966, *MNRAS*, 133, 67
- Duncan A. R., Haynes R. F., Jones K. L., Stewart R. T., 1997, *MNRAS*, 291, 279
- Gaensler B. M., Dickey J. M., McClure-Griffiths N. M., Green A. J., Wieringa M. H., Haynes R. F., 2001, *ApJ*, 549, 959
- Gray A. D., Landecker T. L., Dewdney P. E., Taylor A. R., 1998, *Nat*, 393, 660
- Gray A. D., Landecker T. L., Dewdney P. E., Taylor A. R., Willis A. G., Normandeau, M., 1999, *ApJ*, 514, 221
- Han J. L., Beck R., Berkhuijsen E. M., 1998, *A&A*, 335, 1117
- Haverkorn M., Katgert P., de Bruyn A. G., 2000, *A&A*, 356, L13
- E. M., Krause, M., & Klein, U.
- Koo B.-C., Heiles C., Reach W. T., 1992, *ApJ*, 390, 108
- Minter A. H., Spangler S. R., 1996, *ApJ*, 458, 194
- Naghizadeh-Khouei J., Clarke D., 1993, *A&A*, 274, 968
- Peebles P. J. E., 1984, *ApJ*, 277, 470
- Scheuer P. A. G., Hannay J. H., Hargrave P. J., 1977, *MNRAS*, 180, 163
- Sokoloff D. D., Bykov A. A., Shukurov A., Berkhuijsen E. M., Beck R., Poezd A. D., 1998, *MNRAS*, 299, 189 (Err., *MNRAS*, 303, 207, 1999)
- Subramanian K., 1999, *Phys. Rev. Lett*, 83, 2957
- Sveshnikov A. A., ed., 1965, *Problems in Probability Theory, Mathematical Statistics and Theory of Random Functions*. Nauka, Moscow (English translation: 1968, W. B. Saunders, Philadelphia)
- Tennekes H., Lumley J. L., 1982, *A First Course in Turbulence*. MIT Press, Cambridge, Mass.
- Uyaniker B., Fürst E., Reich W., Reich P., Wielebinski R., 1998, in Breitschwerdt D., Freyberg M. J., Trümper J., eds, *The Local Bubble and Beyond*. Springer, p. 239.
- Uyaniker B., Fürst E., Reich W., Reich P., Wielebinski R., 1999a, *A&AS*, 138, 31
- Uyaniker B., Reich W., Fürst E., Reich P., Wielebinski R., 1999b, in Taylor A. R., Landecker T. L., Joncas G., eds. *New Perspectives in the Interstellar Medium*. ASP Conf. Ser. 168, San Francisco, p. 82
- Wardle J. F. C., Kronberg P. P., 1974, *ApJ*, 194, 249
- Wieringa M. H., de Bruyn A. G., Jansen D., Brouw W. N., Katgert P., 1993, *A&A*, 268, 215
- Zeldovich Ya. B., Ruzmaikin A. A., Sokoloff D. D., 1990, *The Almighty Chance*. World Sci., Singapore